LBL-12015
Preprint

Lawrence Berkeley Laboratory
UNIVERSITY OF CALIFORNIA

Materials & Molecular
Research Division

Submitted to Wear

EROSION OF ELEVATED TEMPERATURE CORROSION SCALES ON METALS

J.A. Maasberg and A.V. Levy

May 1981

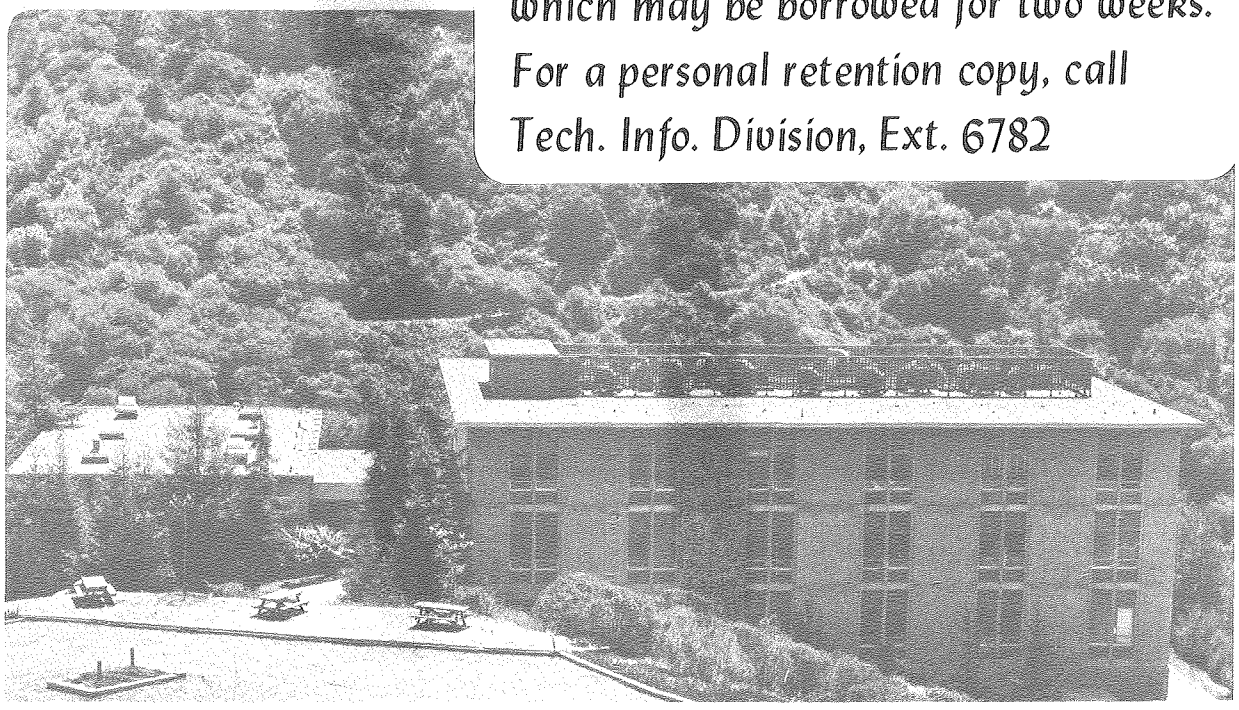

Prepared for the U.S. Department of Energy under Contract W-7405-ENG-48

DISCLAIMER

LBL-12015

EROSION OF ELEVATED TEMPERATURE CORROSION SCALES ON METALS

J. A. Maasberg and A. V. Levy

Materials and Molecular Research Division
Lawrence Berkeley Laboratory
University of California
Berkeley, CA 94720

May 1981

This work was supported by the Director, Office of Energy Research, Office of Basic Energy Sciences, Materials Sciences Division of the U.S. Department of Energy under Contract Number W-7405-ENG-48.

EROSION OF ELEVATED TEMPERATURE CORROSION SCALES ON METALS

J. A. Maasberg and A. V. Levy

Materials and Molecular Research Division
Lawrence Berkeley Laboratory
University of California
Berkeley, CA 94720

ABSTRACT

Combined erosion-corrosion poses a considerable problem to the design of long lifetime metallic components in energy conversion systems. To gain some insight into this problem, scales were formed on stainless steel at elevated temperature and subsequently were eroded at room temperature to determine the nature of the erosion rates and the mechanism of scale removal. Thin corrosion scales were formed on 310 stainless steel and an experimental Fe-18Cr-5Al-1Hf alloy at high temperatures (900° and 980°C) in gas mixtures with various levels of oxygen and combined oxygen-sulfur. The corroded specimens were eroded at room temperature in an air-solid particle stream using 50μm SiC at 60 ms^{-1}. The conditions of the corrosive exposures, the rates of erosion of these scales and the microscopic appearance of the eroded surface were correlated to determine the mechanism of thin scale erosion.

INTRODUCTION

The high temperature environments in advanced energy conversion systems, in particular coal gasifiers, have caused the degradation of metallic components due to the combined actions of particle erosion with high temperature corrosion. Protective oxide layers which form at high temperatures are often damaged by rapidly moving particles, thus leaving metals susceptible to further corrosive damage. This investigation determined the dependence of erosion damage on the corrosion conditions, specimen surface conditions, and the structure of the corrosion product scale. In addition, microscopic examination was used to determine the mechanism of erosion of a thin oxide on a metal formed at an elevated temperature and subsequently eroded at room temperature.

Originally investigated by Finnie[1,2], the removal of material from ductile metals by the erosive action of small angular particles was attributed to a different mechanism than material removed from brittle materials. Brittle materials were determined to erode by a microfracturing of the ceramic, whereas ductile metals erode by a plastic deformation mechanism. Figure 1 shows the impingement angle dependence of the erosion rate for typically ductile and brittle materials and clearly differentiates the behavior of each. Erosion of brittle, thin oxide scales formed in-situ on metals which occurs in coal gasifier environments could be classified as occurring in either a ductile or brittle manner. It was necessary to determine which mechanism is active. An understanding of combined erosion-corrosion could be

achieved by separating the formation of the scale from its erosive removal. In order to accomplish this, the scale was separately formed on the metal and then eroded.

Work by Zambelli[3] has shown that relatively thick (20-100μm) oxide scales on nickel behave in a brittle manner, undergoing hertzian cup-cone and radial fractures to break up the scale upon impact by particles. He reported that the thinner the scale, the more of a contribution the ductile metal substrate made to the erosion behavior. The thin scales that we investigated were expected to behave more like ductile than brittle materials because they were so thin that it was felt that the ductile substrate would be the governing factor. This work disproved that premise.

EXPERIMENTAL PROCEDURE

The high temperature corrosion of 310 stainless steel (310SS) makes it a much used material in highly corrosive areas of energy conversion systems. Because of this, it was selected for this project to study the combined effects of erosion and corrosion. For comparison, an alumina scale forming experimental Fe-18Cr-5Al-1Hf alloy was included in a few of the tests. Corroding gas mixtures were selected to be representative of conditions encountered in coal gasification systems.

The specimens were alloy coupons approximately 2.54 x 1.90 x 0.318 cm, with a small hole drilled toward one side in order to attach them to the support in the corrosion furnace. The specimens were suspended in various gas mixtures at temperatures of 900° and 980°C for a period of 100 hours in order to develop a continuous surface scale. The following corrodant mixtures were used:

air	$P_{O_2} = 10^{-15} + P_{S_2} = 10^{-8.5}$
$P_{O_2} = 10^{-15}$	$P_{O_2} = 10^{-16.9} + P_{S_2} = 10^{-6}$
$P_{O_2} = 10^{-16.5}$	$P_{O_2} = 10^{-17.4} + P_{S_2} = 10^{-7}$
$P_{O_2} = 10^{-15} + P_{S_2} = 10^{-6}$	

They were made by mixing H_2, H_2S, H_2O and argon in the test furnace.

The gas compositions were selected to represent the wide range of conditions that could occur in coal gasifiers forming different types of scales. For example, oxidizing the 310SS in air results in an oxide scale whose morphology and, hence, erosion behavior should differ from

an oxide scale formed at an oxygen partial pressure of 10^{-15} atmos. In the combined oxidation-sulfidation tests, partial pressure combinations were selected based on the thermodynamic equilibrium stability diagrams that would result in a protective oxide and no sulfide, mixtures near the oxide-sulfide formation dividing line and a mixture in the sulfide forming region of the stability diagram. In order to determine whether an oxide scale that had formed not in competition with sulfur could provide erosion protection after a subsequent exposure to combined oxygen and sulfur, some pre-oxidized specimens were prepared. Burnished and as-received specimen surface conditions were studied.

Erosion testing was performed at room temperature on previously formed corrosion scales. The air-blast erosion tester is illustrated in figure 2. 50μm size SiC particles carried by air at 60 ms^{-1} were used to erode away the scales on the test coupons without eroding the base metal. The weight loss of the specimens was measured intermittently during erosion and the resulting weight losses were compared to determine the erosion behavior. Generally, the weight loss after 0.3g of SiC indicated the steady state erosion rate of the scale. The metal substrate was reached after eroding with 0.3g to 1.0g of SiC. The threshold period of no erosion of the metal substrate was completed only after 3-5g of erodent was used. Since no weight loss due to erosion occurred on an unoxidized 310SS specimen after erosion by 1g of erodent, the weight loss on the corroded specimens is due entirely from the scale. Figure 3 shows a before-after cross section of an oxidized 310SS specimen eroded with 1.2g of SiC. Note that the scale was removed, yet the metal substrate was unaffected.

Microstructural examinations of the specimens were performed by cross sectioning with a diamond saw and mounting them in bakelite, using Klarmount about the face of the specimen in order to avoid rounding off the scale edge. Cross sections were ground on abrasive paper to 600 grit, polished with 5 and 1 m cerium oxide polishing compound. Analysis of the corrosion scale was performed by optical microscopy, scanning electron microscopy with x-ray fluorescence analysis, and x-ray powder diffraction.

Results

Figure 4 shows the 310SS specimens after the elevated temperature corrosion had occurred yet prior to erosion testing of the scales that had formed. The scales were generally continuous; only those exposed to the $P_{O_2} = 10^{-16.9} + P_{S_2} = 10^{-6}$ gas mixture formed a visible sulfide formation on the surface. No distinct areas of sulfide could be found, microscopically or analytically, on any of the other specimens that were exposed to sulfur bearing gases. The specimens with the visible sulfide formations were not erosion tested. Figure 5 shows a typical specimen after being eroded. The removal of the thin, 3-6 m, scale by the eroding particles impacting at 90^{o} caused a circular lightened area to occur on the specimen. Weight losses measured were generally near a milligram.

Scales in Oxidizing Atmospheres

Table 1 presents the results of the erosion tests on the oxidized 310SS specimens. It can be seen that increasing the oxidation temperature from 900°C (1650°F) to 980°C (1800°F) increased the thickness of the scale formed in air from 2.5μm to 15μm. The thinner scale eroded at a lower rate, 0.003g/g erodent. This follows the trend found by Zambelli[3] where thinner scales on metal substrates erode at a lower rate than thicker scales.

The erosion that occurred on the scale formed at the low P_{O_2} was less than that formed in air. The erosion that occurred at a 90° impingement angle was more than that which occurred at a 30° impingement angle, indicating that the scale eroded like a brittle material even though it was very thin and was on a ductile metal substrate. No apparent difference in erosion behavior resulted from burnishing the specimens prior to oxidizing them. It is known that burnishing does extend the straight oxidation resistant life of specimens not subsequently exposed to an eroding environment.[4] No difference in erosion behavior was measured for specimens oxidized at the two different low oxygen partial pressures used.

The amount of erosion only approximately doubled after four times the amount of particles had been used, 0.3g compared to 1.2g of erodent. This indicates that the amount of erosion per unit of particles decreased with increasing erosion. Figure 6 shows this more clearly. The curve plots material loss for each subsequent 0.1gm of eroding SiC particles. The higher initial slope of the curves

indicates a high rate of erosion; when the curves become straight, a steady state erosion condition has been reached where each 0.1g of particles causes the removal of the same weight of target scale. When the lower curves become flat, all of the scale has been removed.

Since the threshold period for the initiation of erosion in the ductile metal substrate is approximately 5g of material[3], no metal was observed to be removed in these tests. Figure 3 shows this; the internal oxidation just below the scale-metal interface is intact in the eroded specimen, indicating that only the Cr_2O_3 scale in the upper photo was removed in the erosion process.

Figure 6 compares the erosion behavior of air oxidized and low P_{O_2} oxidized 310SS and the erosion of an alumina scale which was formed on an experimental FeCrAlHf alloy. The low P_{O_2} atmosphere developed a much more erosion resistant scale that averaged 4μm thick. The air oxidized specimen lost more total weight than the low P_{O_2} formed scale because it had a thicker scale to start with. Comparing the early portions of the erosion of each scale, up to 0.4g of particles, shows a much higher rate of loss of the air oxidized scale. The difference in morphology that accounts for this behavior is still under investigation. There was no apparent difference in the erosion behavior of scales formed at two different, low P_{O_2} levels.

The erosion rate of the alumina scale was significantly less than that of the chromia scale, as shown in figure 6. Figure 7 shows the cross section of the chromia and alumina scales. The dark colored internal oxides below the chromia scale are SiO_2. They form a discontinuity at the scale-metal interface that reduces the erosion resistance

of the scale by deteriorating the bond between the scale and the metal substrate. The alumina scale, by comparison, has no alternate oxide at the scale-metal interface. The alumina scale continues into the base metal in the form of pegs or fingers of alumina, markedly improving the bond between the scale and substrate. This structure is promoted by the presence of the hafnium in the alloy and is known to also enhance the corrosion resistance of the alloy.[5]

Scales in Oxidizing-Sulfidizing Atmospheres

The scales formed in the presence of both oxygen and sulfur that were erosion tested had no discernible sulfides in them as determined by energy dispersive x-ray analysis in the scanning electron microscope (SEM), and by powder x-ray diffraction. However, their formation in the presence of sulfur did reduce their erosion resistance to a level below that of straight oxidized scale. Figure 8 shows the effect of combined oxidation-sulfidation on the chromia scale and figure 9 shows the effect on the alumina scale. The attempt to form a more erosion resistant scale on the 310SS by first forming an oxide of Cr_2O_3 that was not in competition with sulfur and subsequently exposing the specimen to a combined oxidizing-sulfidizing atmosphere had some success, as can be seen by the pre-oxidized curve in figure 8.

The greater erosion resistance of the alumina scale formed in a straight oxidizing atmosphere compared to that formed in a combined oxidizing atmosphere, shown graphically in figure 9, can be related to the scales' microstructures in figure 10. The reduction in the amount

of pegging shown in the lower photo, the oxidized-sulfidized specimen, reduces the bond between the scale and the substrate and the erosion increases. It was observed that no difference in erosion rate occurred as the result of differences in the particle impingement angle between 30^{o} and 90^{o}. A decided difference was measured in straight oxidized specimens (see Table 1).

The increased erosion rate of the 2.5-5μm thick chromia scale that was formed in the presence of sulfur compared to a straight oxidized chromia, as shown in figure 8, can be at least partially related to observed differences in their microstructure. The thickness of both of the scales was essentially the same and did not contribute to the difference observed in their erosion behavior. Figure 11 shows that an almost continuous SiO_2 scale formed along the scale-metal interface of the oxidized-sulfidized specimen while only near perpendicular fingers of SiO_2 formed in the straight oxidized 310SS. The resulting deterioration of the oxidized-sulfidized scale-metal interface increased the erosion role of the scale. Figure 12 is a sketch of how the morphology of the scale-metal interface affected the erosion behavior of the scales. The first picture represents the pegging type of structure found in the straight oxidized alumina scale. The second and third figures depict the straight oxidized chromia scale and the fourth figure represents the combined oxidized-sulfidized chromia scale.

The effect of pre-oxidizing the 310SS on the scale-metal interface morphology is shown in figure 13. The primary difference is the morphology of the SiO_2 internal oxides. By pre-oxidizing, the SiO_2 that

forms essentially parallel to the scale-metal interface is almost eliminated, with a consequent improvement in the erosion resistance.

Mechanism of Erosion

In order to determine the mechanism by which the thin scales eroded, the technique of sequential erosion used in the investigation of the erosion of NiO scales formed on nickel[3] was used. After each few particles had impacted the surface, the specimen was removed from the erosion tester and the eroded surface observed in the SEM. Figure 14 shows the scale surface after a few particle impacts had occurred in the area under observation. The small crystallite surfaces have not yet been impacted. The darker appearing areas representing less than 50% of the total area shown have received at least one SiC particle impact. Figure 15 shows one of the impacted areas at a higher magnification. In the left center of the photo some smeared crystallites can be seen, indicating that plastic deformation of the immediate scale surface had occurred. The flat areas at different planes to one another indicate that cracks had formed at various angles but near parallel to the plane of the scale and pieces of scale had been chipped out. Even though the scale is only approximately 4μm thick, the cracks that resulted in chip removal occurred in the scale above the scale-metal interface. The remaining material in the chipped areas is Cr_2O_3 and not base metal.

DISCUSSION

The principal finding of this investigation is that both the chromia and alumina scales formed in-situ on aluminum and/or chromium containing alloys behave in a brittle manner when eroded, even though they were as thin as 2.5μm and were generally intimately bonded to the ductile metal substrate. They behaved as other ceramic materials do in gas-solid particle erosion environments, losing material in sequentially removed layers of scale by a cracking and chipping mechanism. While the scale-metal interface appeared to play an important role in determining the erosion rate with greater bonding resulting in lower erosion rates, the scale was not removed by separation at the scale-metal interface. Also, the scale of the straight oxidized specimen eroded at higher rates at an impingement angle of 90^{o} than at 30^{o}. This behavior is typical of brittle materials. The difference in the amount of erosion as a function of impact angle was not observed in the scales formed in oxidizing-sulfidizing atmospheres. This anomaly indicates that the weakened scale formed in the presence of sulfur may be eroding at such a high rate as to not provide effective crack resistance at shallow impingement angles where the crack formation stresses are not as great as those which occur nearer 90^{o} impingement angles.

The behavior of the thin, brittle scale formed in-situ on the ductile substrate was much more independent of the substrate than had been expected. It was initially thought that the erosion behavior of the thin scale would be modified by the ductile nature of the substrate because of the trend of thinner scale having a lower erosion rate in

the work of Zambelli.[3] The thicker (.015μm) chromia scale formed in air eroded at a rate 3 times faster than the thinner (2.5μm) chromia scale formed in a low P_{O_2} gas atmosphere. This indicates that some degree of transfer of the particle impact stresses into the substrate had occurred. The somewhat more porous morphology of the air oxidized specimens may also have contributed to the difference. However, both scales eroded at rates representative of brittle materials rather than ductile ones. This implies that chromia and alumina scales on alloys will undergo rapid erosion when they form in a combined erosion-corrosion environment.

The erosion resistance of the scales depended to a strong degree on the conditions under which the scales were formed. Oxides formed more slowly at low partial pressures of oxygen eroded much more slowly than those that were formed in air. While it was not possible to discern any significant difference in the morphology or composition of the scales to account for this difference, a recent work by Kofstad and Tillerad[6,7] may shed some light on the differences. They found that chromium oxide formed on pure chromium at 1000°C had fewer cracks when formed at low P_{O_2} than when formed in air. They also found that the low P_{O_2} formed oxide had large, sintered grains of higher integrity near the scale-metal interface and small, more porous grain structure at the gas-scale interface. The smaller, more porous grain structure that formed in air could be more susceptible to erosion, based on Zambelli's work on NiO.[3] In Zambelli's work, the porous scale formed below the higher integrity larger grains, but the higher erosion rate occurred in the small grain, more porous structure. Also the presence of more erosion

resistant Cr_2O_3 grains near the scale-metal interface compared to the more porous grains further out in the scale could account for the curves of erosion vs. amount of particles showing a decreasing amount of erosion with increasing amounts of particles.

It was also determined by Kofstad that the ability of the scale to deform plastically goes up significantly as the P_{O_2} decreases. This could also have improved the erosion resistance of the scale formed at low P_{O_2}. While Kofstad's work was done with pure Cr and this work with 310SS, the physical behavior of the Cr_2O_3 appears to be similar. More work is necessary to verify this.

Kofstad also observed that the Cr_2O_3 scale buckled as it grew laterally as well as in the thickness direction, causing void areas to appear midway in the scale. These blisters would present a preferred target to the eroding particles, accounting for the initial areas of erosion. Also, increased Cr transfer across the void area could take place because of the high CrO vapor pressure that occurs near 1000°C. This could cause an enrichment in the iron content of the scale beneath each buckled blister which would account for the iron enriched areas observed in the areas beneath the initial eroded blisters in the sequential erosion of the scale on the 310SS.

The temperature at which the scale formed, 900°C and 980°C, also appeared to have a significant effect on the erosion behavior of the scale. Thus, the nucleation and growth mechanism as well as the scale growth rate affects the erosion rate of the scale.

The presence of sulfur in the corroding gas markedly decreased the erosion resistance of the resulting scale to below that of the straight

oxygen produced scale even though no direct evidence of sulfur was found in the scale. This indicates that the morphology of the scale is subtley modified in combined erosion-corrosion.

In work by Yurek[8] on the combined oxidation-sulfidation of pure Cr he observed that at a $P_{O_2} = 10^{-10}$ atmos nucleii of chromium sulfide formed on the scale-metal interface while no sulfide formed in the scale. The reduction in the integrity of the scale-metal interface of the 310SS by the same or a similar mechanism may have increased the erosion rate of the oxidized-sulfidized specimens. Specimens from the corrosion conditions that produced visible sulfide scale nodules on the surface were not eroded because of the obvious loss of surface integrity.

The relation between the composition and morphology of the scale-metal interface and the erosion rate of the scales tested was unexpected. The degree and orientation of internally oxidized SiO_2 near the scale-metal interface most directly related to the erosion rate of the scale. It was not determined why the large amounts of parallel to the interface oriented SiO_2 occurred in the combined oxidized-sulfidized specimens compared to the lower quantity and perpendicular to the interface orientation of the SiO_2 formed in the straight oxidized specimens. However, the effect of the difference on the erosion behavior of the chromia scale was marked.

The SiO_2 became an interface contaminant that may have blocked effective transfer of particle impact deformation stresses from the scale to the substrate. Such an occurrence would increase the force effect of the particles on the scale, enhancing their ability to crack the scale. The SiO_2 did not appear to directly reduce the adherence of

the scale which could result in the pieces of scale that were removed leaving from the scale-metal interface in full scale thickness pieces. The scale was removed by sequential removal of layered chips of scale.

The difference in the erosion rates of the chromia and alumina scales appears to be related to at least three factors. The basic strength of the alumina was greater than that of the chromia in erosion type loading. The absence of a contaminant like the SiO_2 in the chromia scale specimens and the pegs of alumina extending into the substrate are the other two factors involved; they improved the scale-metal interface. Figure 12 shows the relationship between scale-metal interface morphology and erosion behavior graphically. The reason why such a relationship exists when erosion did not take place from the interface can only be speculated at this time.

Preventing the formation of the parallel to the interface contaminant by pre-oxidizing the chromia specimens did improve the erosion resistance of the specimens; this reduces the tendency toward erosion depicted in figure 12. Reducing the pegging of the alumina scale by combined oxidation-sulfidation, compared to straight oxidation reduced the erosion resistance of the alumina scale, which also supports the trend shown in figure 12. In the case of the alumina, the pegging may increase the transfer of stress from the impacted scale to the substrate, thereby increasing the erosion resistance, compared to the chromia scale where parallel SiO_2 decreased the transfer of stress which decreased the erosion resistance.

CONCLUSIONS

1. The thin chromia and alumina scales that form, in-situ, on aluminum and/or chromium containing alloys erode in a brittle manner, losing material by a cracking and chipping mechanism that sequentially moves through the scale thickness. Scale removal did not occur by separation directly from the scale-metal interface.
2. Low P_{O_2} containing gases form more erosion resistant scales than those formed in air.
3. The presence of sulfur in the corroding gases markedly increases the erosion rate of the chromia and alumina scales even though the presence of sulfur in the scales was not measureable.
4. Alumina scales with pegging into the substrate had greater erosion resistance than chromia scales. Greater extent of pegging resulted in greater erosion resistance.
5. The presence of SiO_2 internal oxides at the scale-metal interface of the chromia scales increased the erosion rate of the scale as their quantity and orientation parallel to the scale-metal interface increased.
6. Thinner scales eroded at a lower rate than thicker scales formed in the same air atmosphere indicating that the ductile substrate does absorb some of the kinetic energy of the eroding particles.

ACKNOWLEDGEMENT

We wish to acknowledge and express our appreciation to Professor David Whittle for his valuable discussions and Larry Lapides for his experimental assistance.

This work was supported by the Director, Office of Energy Research, Office of Basic Energy Sciences, Materials Sciences Division of the U.S. Department of Energy under Contract Number W-7405-ENG-48.

References

1. I. Finnie, J. Wolak, Y. Kabil, "Erosion of Metals by Solid Particles", J. of Materials, 2 (3), September 1967.
2. I. Finnie, "Erosion of Surfaces by Solid Particles", Wear, 3 (1960).
3. G. Zambelli, A. Levy, "Particulate Erosion of NiO Scales", Wear, 68 No. 3, p. 305-331, 1981.
4. R. Perkins, "Development of Alloys for Use in Coal Derived Gases"; Proceedings NACE International Conference on High Temperature Corrosion, San Diego, California; March, 1981.
5. D. P. Whittle and J. Stringer, Phil. Transactions, Royal Society London; A295 309 (1979).
6. K. P. Tillerad and P. Kofstad, J. Electrochemical Society, 127 (1980) 2397.
7. P. Kofstad and K. P. Tillerad, ibid, 127 (1980) 2410.
8. M. Labranceh, M. Gomez, G. J. Yurek; "Early Stages of the Oxidation of Chromium in H_2-H_2O-H_2S Gas Mixture"; Proceedings NACE International Conference on High Temperature Corrosion; San Diego, California; March 1981.

TABLE 1

Air Oxidation of 310 S.S.

Surface	°C	Log P_{O_2}	Scale thickness (μm)	90° weight loss after 0.3g SiC	90° weight loss after 1.2g SiC	30° weight loss after 0.3g SiC	30° weight loss after 1.2g SiC
As Received	900	air	2.5	0.9	1.6	0.6	1.2
	980	air	15	2.7	4.5	2.1	3.9
Burnished	900	air		0.5	1.05		
	980	air		3.4	5.6		

Low P_{O_2} Oxidation of 310 S.S.

	900	-15		0.4	0.7		
As Received	900	-15	4	0.3	0.6	0.1	0.3
	900	-16.5		0.4	0.7		
	980	-16.5		0.4	0.7		

Figures

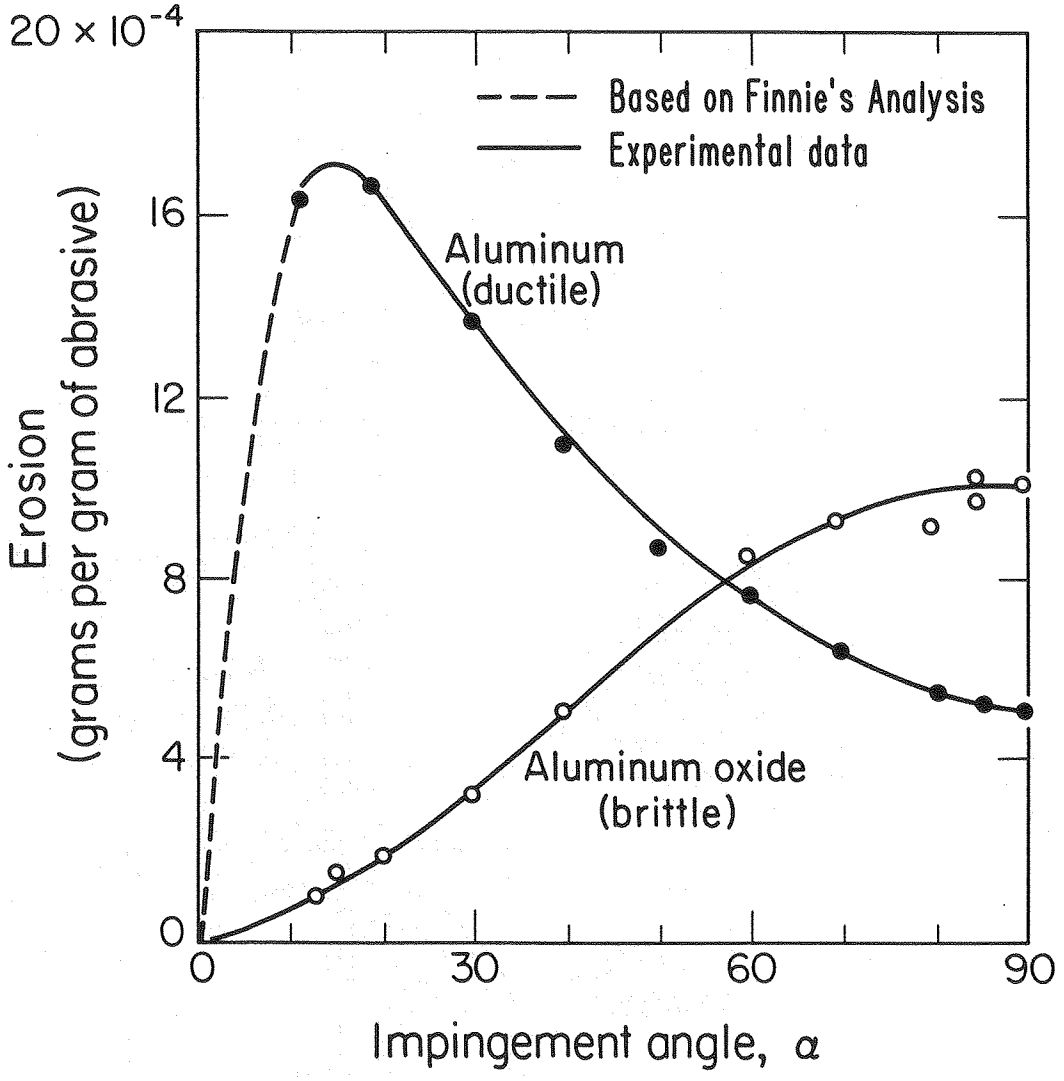

Fig. 1

XBL 793-974

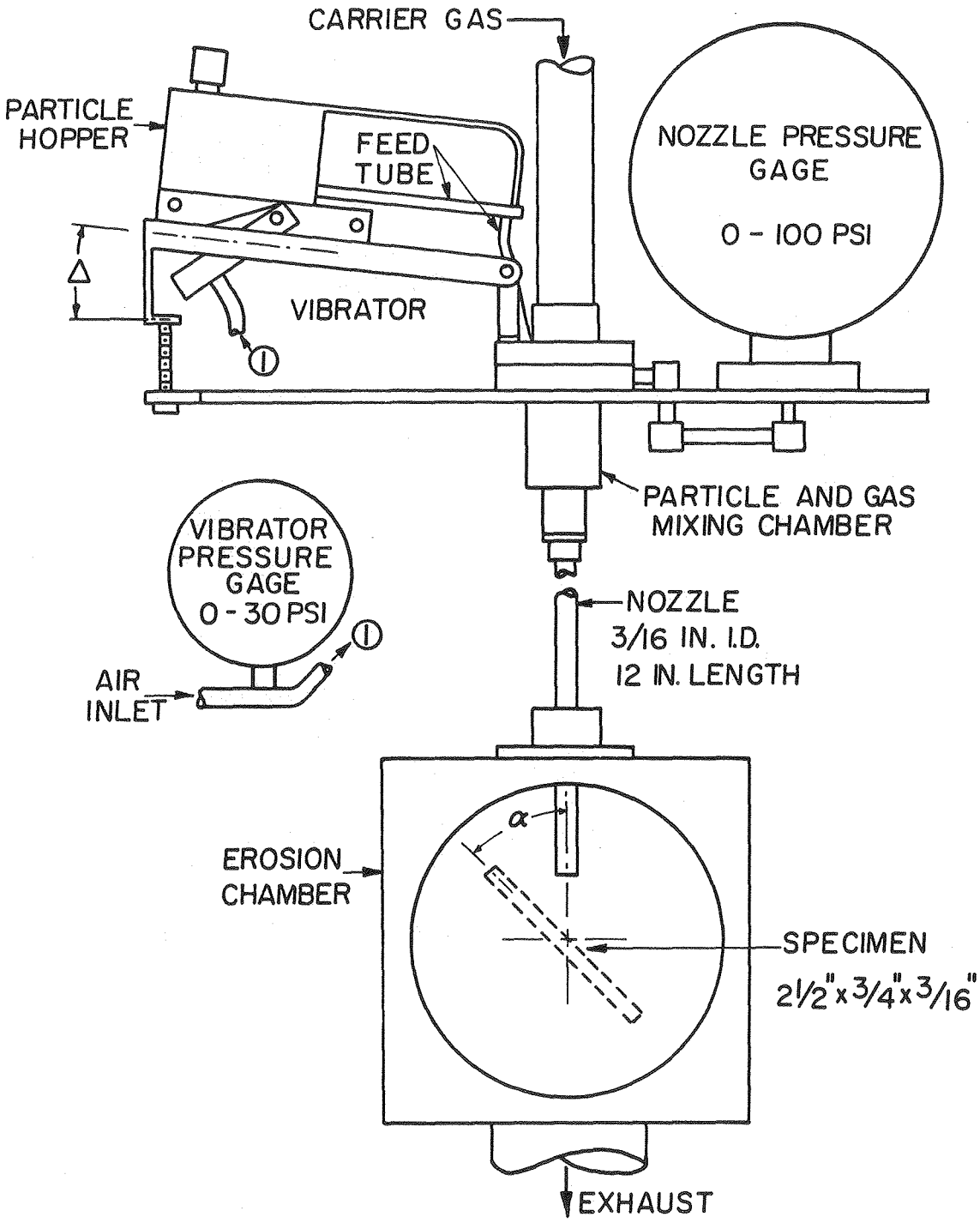

XBL775-5525

Fig. 2

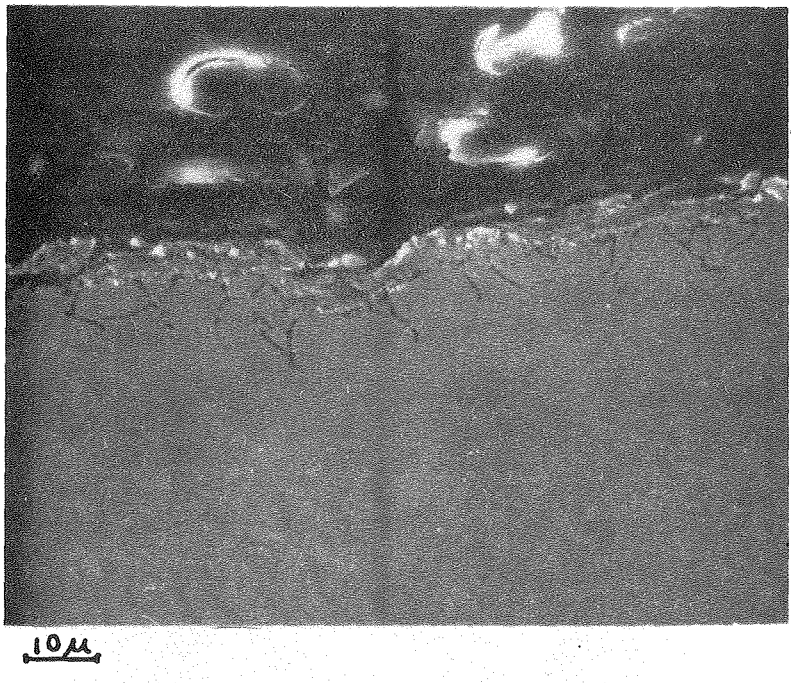

Type 310 S.S. Oxidized: Log P_{O_2} = -15, 1650°F

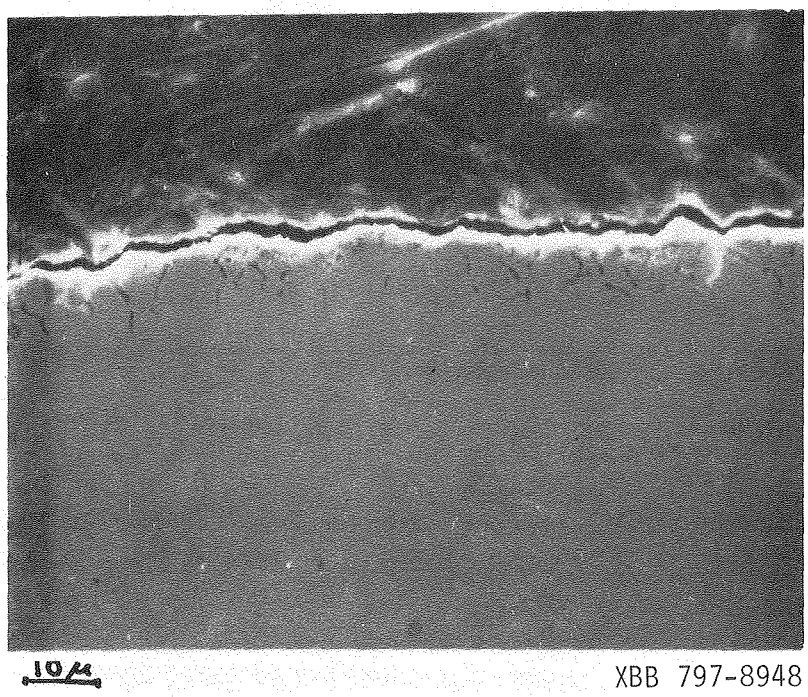

XBB 797-8948

Fig. 3 Type 310 S.S. Oxidized: Log P_{O_2} = -15, 1650°F
Eroded: 90° incidence angle

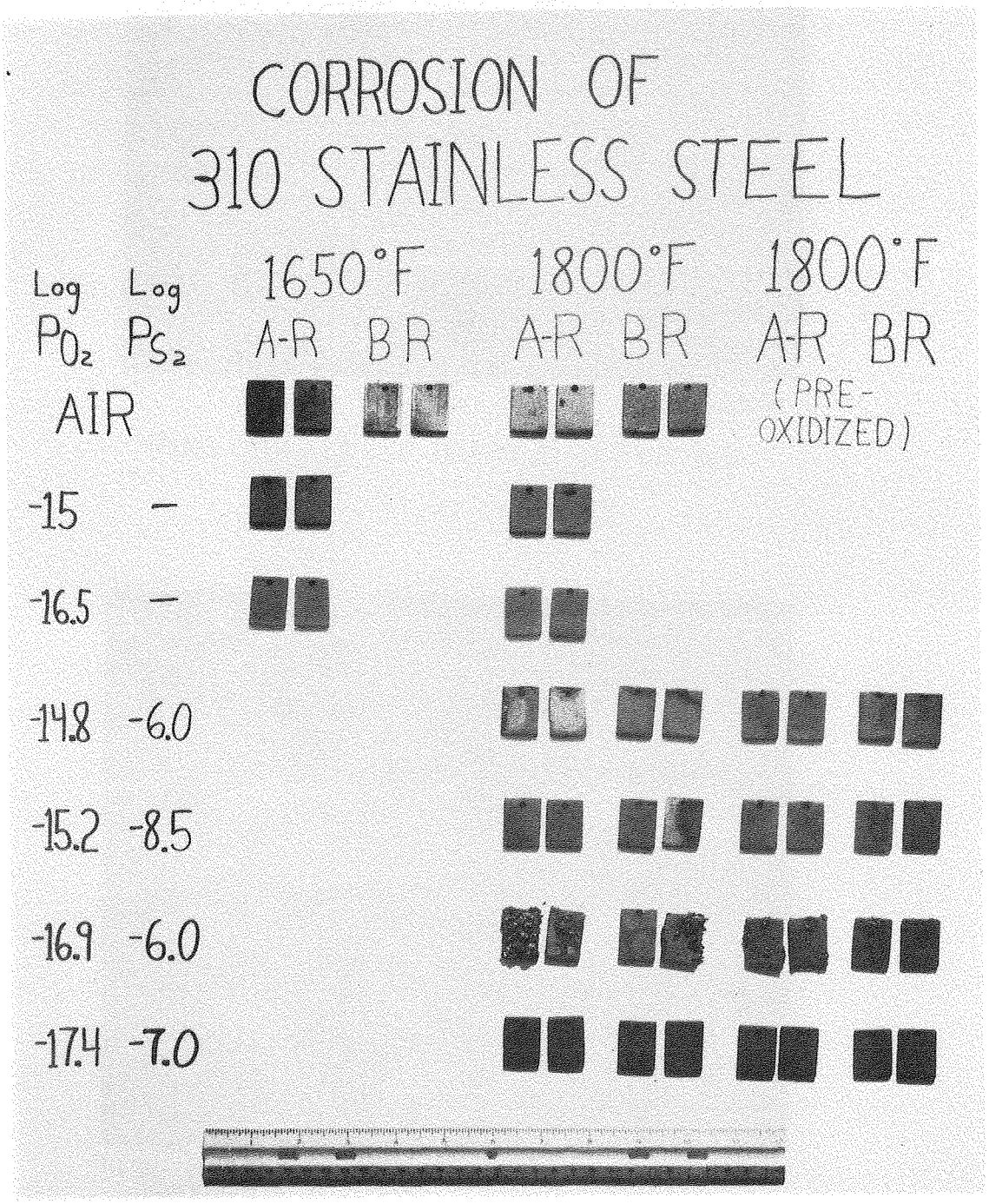

Fig. 4

CBB 791-349

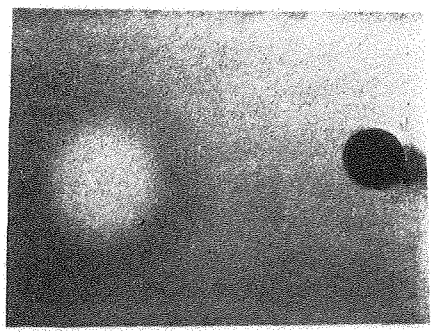

Erosion Specimen: Type 310 S.S.

Preoxidized: Log P_{O_2} = -15, 1800°F

Oxidized - Sulfidized: Log P_{O_2} = -15, Log P_{S_2} = -9, 1800°F

Fig. 5

CBB 797-8941

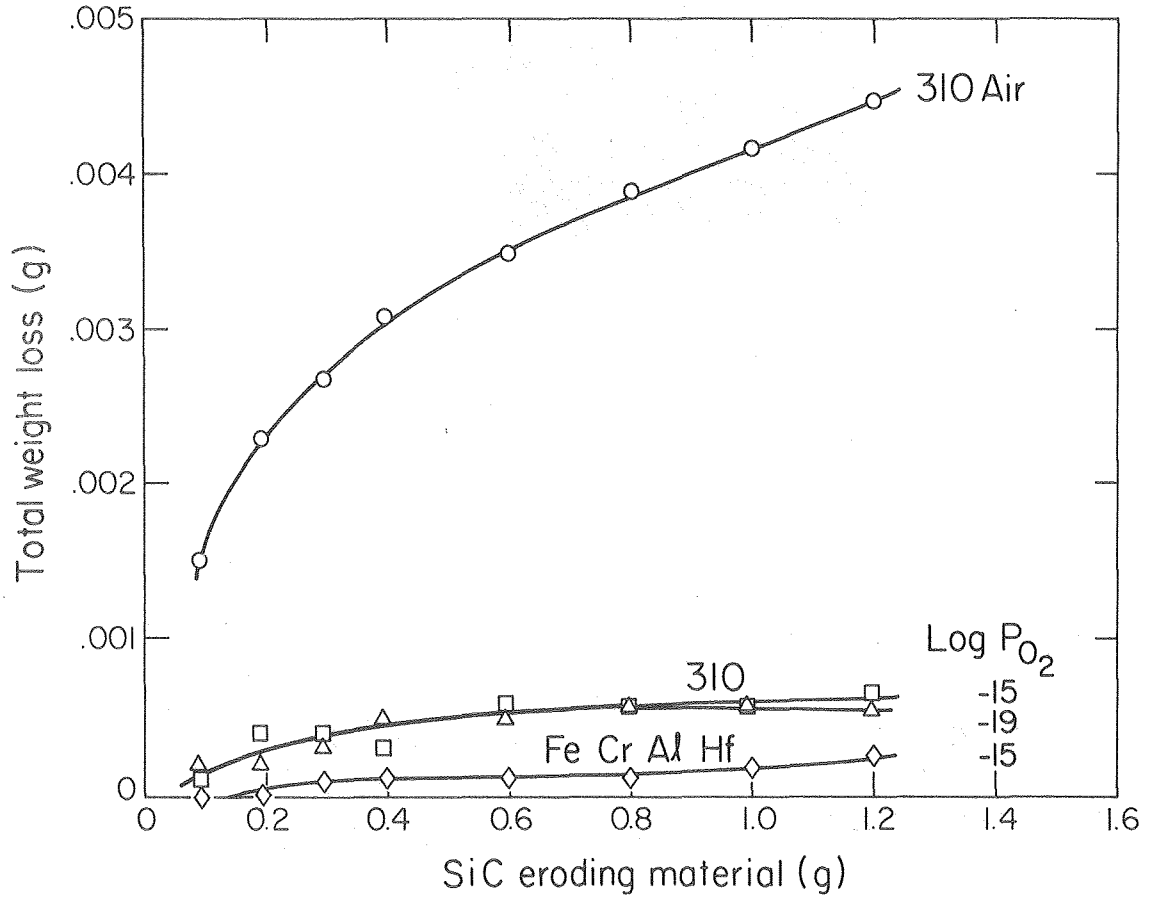

Fig. 6

XBL 793-803

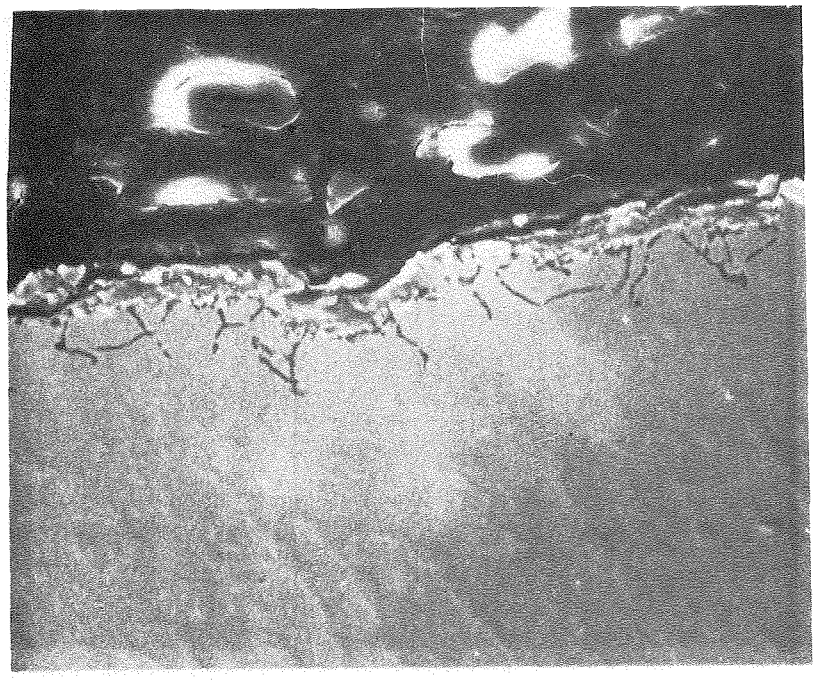

Type 310 S.S. Oxidized: Log P_{O_2} = -15, 1650°F

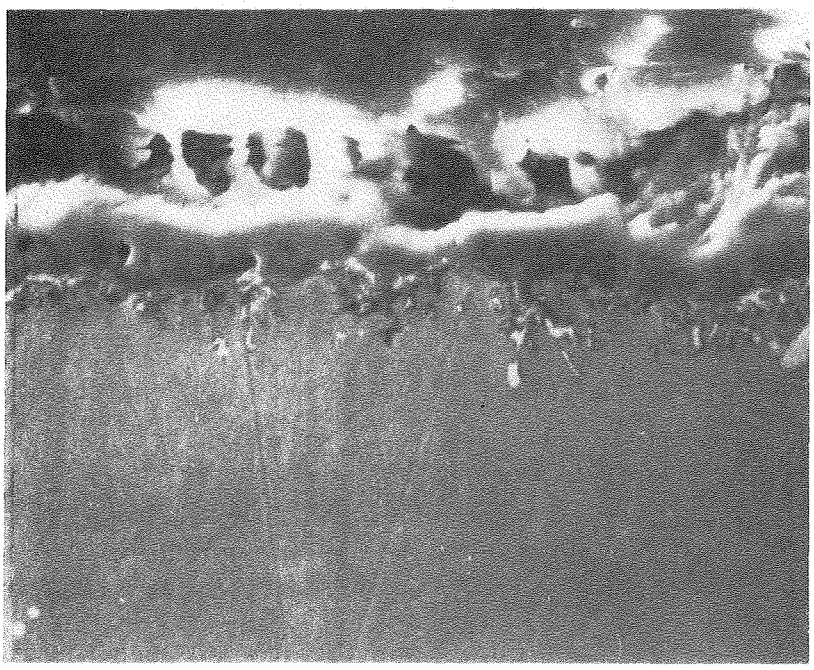

Fig. 7 Fe 18Cr 5Al 1Hf Oxidized: Log P_{O_2} = -15, 1800°F

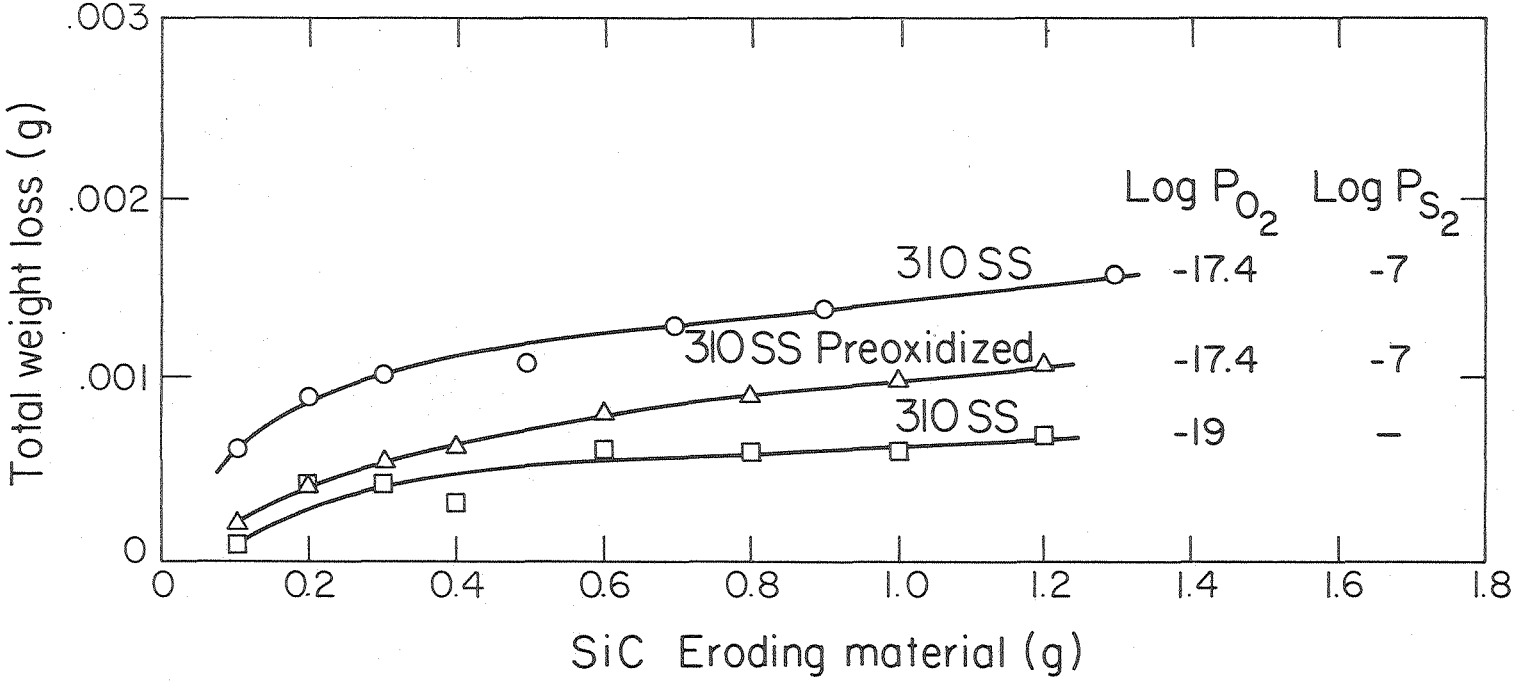

Fig. 8

XBL 793-805

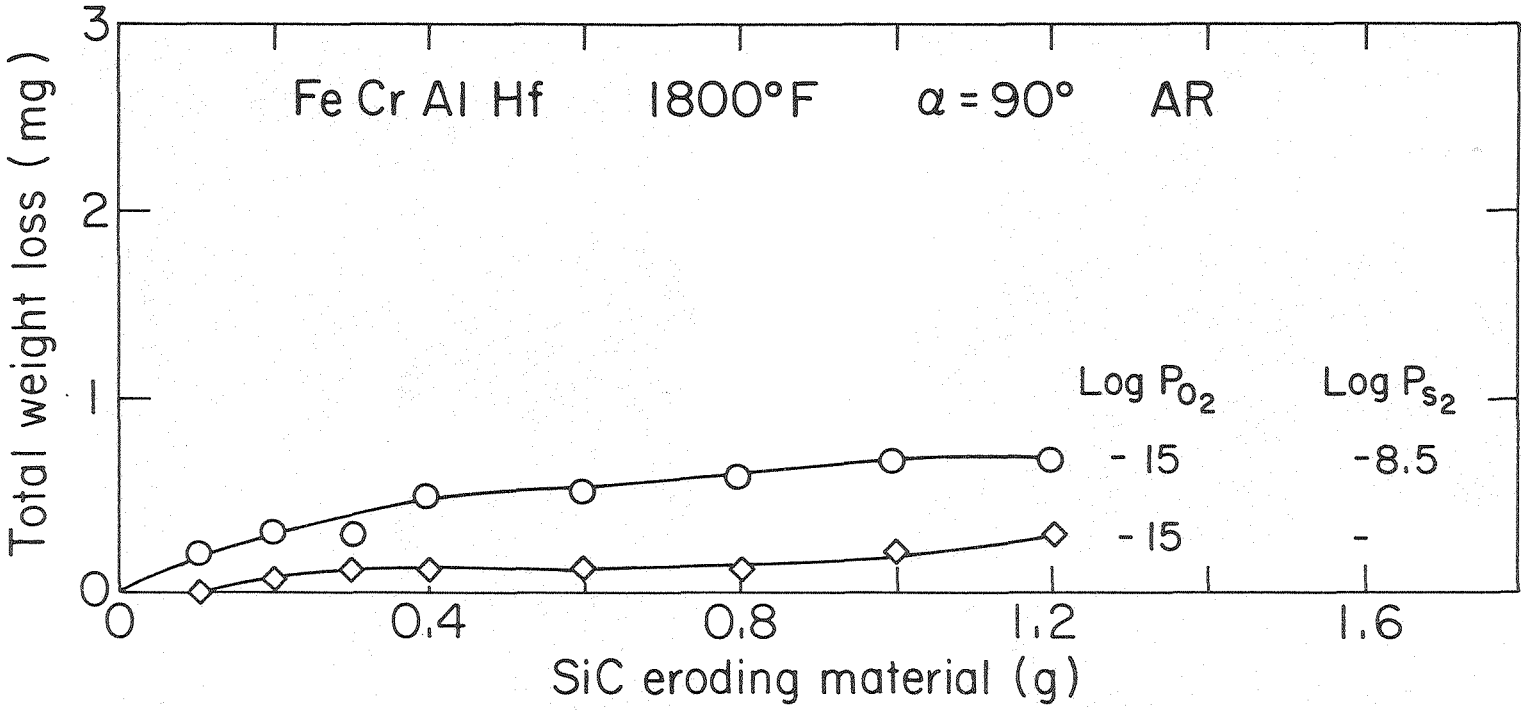

Fig. 9

XBL 801-95

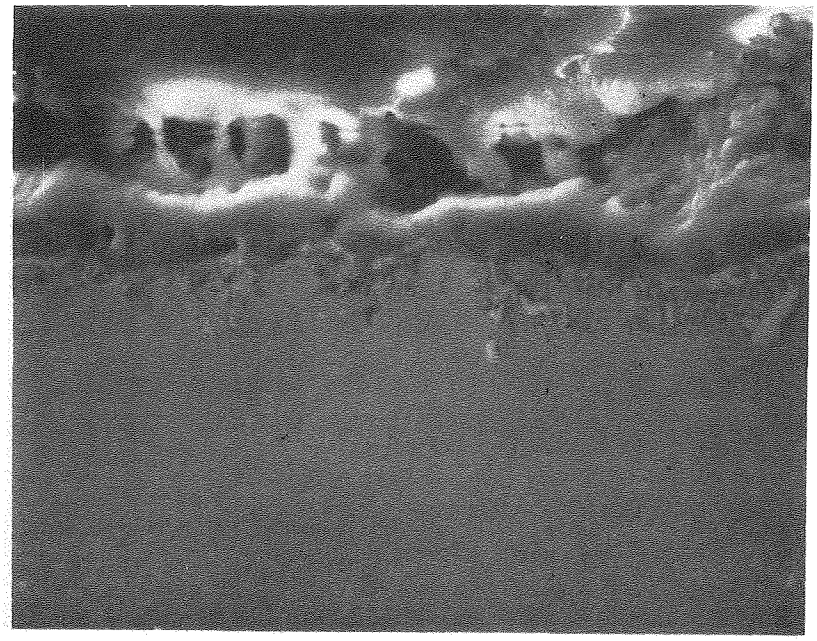

5 μ

Fe 18Cr 5Al 1Hf Oxidized: Log P_{O_2} = -15, 1800°F

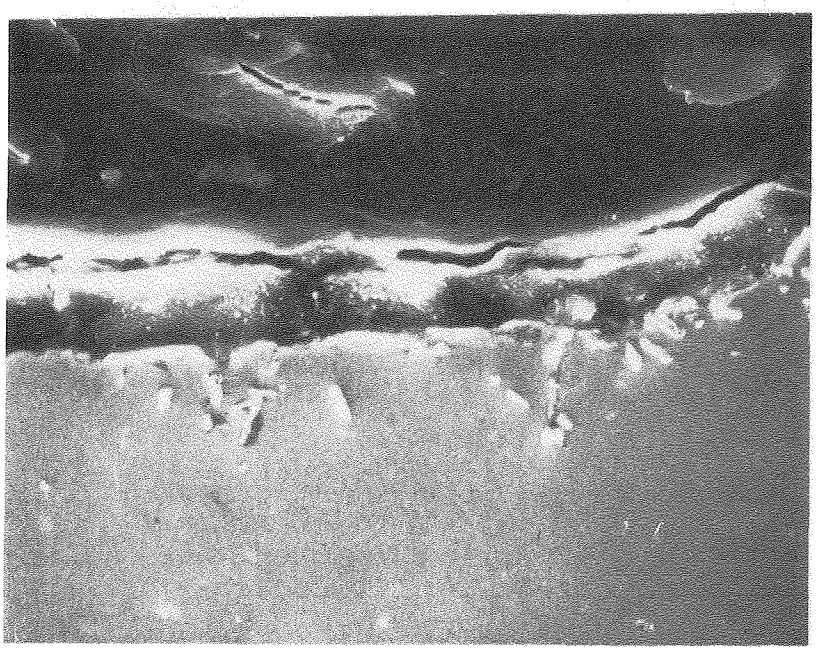

XBB 797-8946

5 μ

Fig. 10 Fe 18Cr 5Al Hf

Oxidized - Sulfidized: Log P_{O_2} = -15, Log P_{S_2} = -8.5, 1800°F

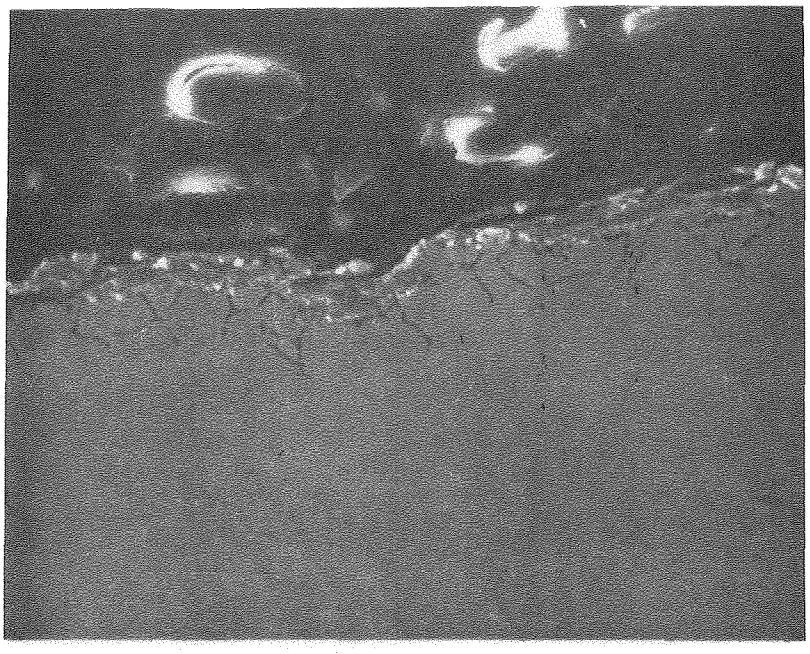

Type 310 S.S. Oxidized: Log P_{O_2} = -15, 1650°F

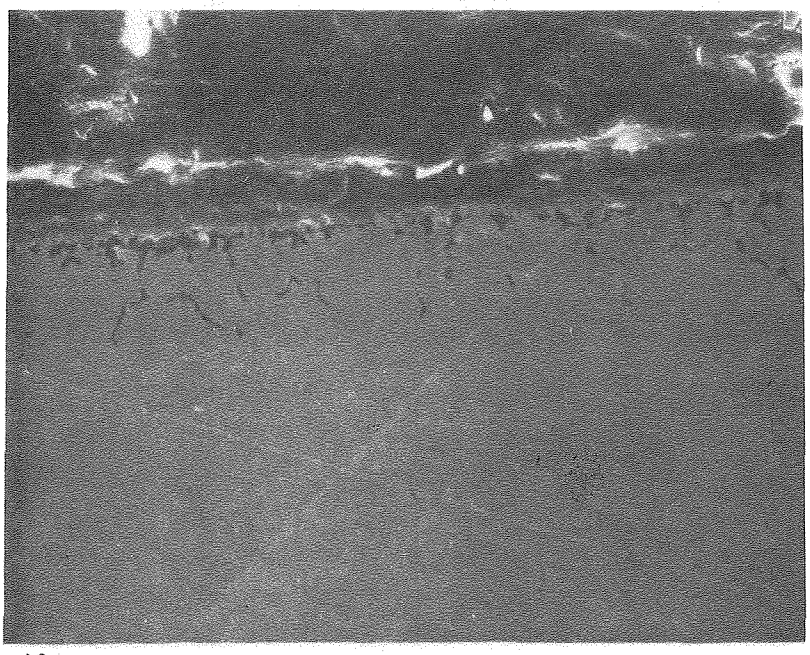

XBB 797-8951

Fig. 11 Type 310 S.S.

Oxidized - Sulfidized: Log P_{O_2} = -15, Log P_{S_2} = -6, 1800°F

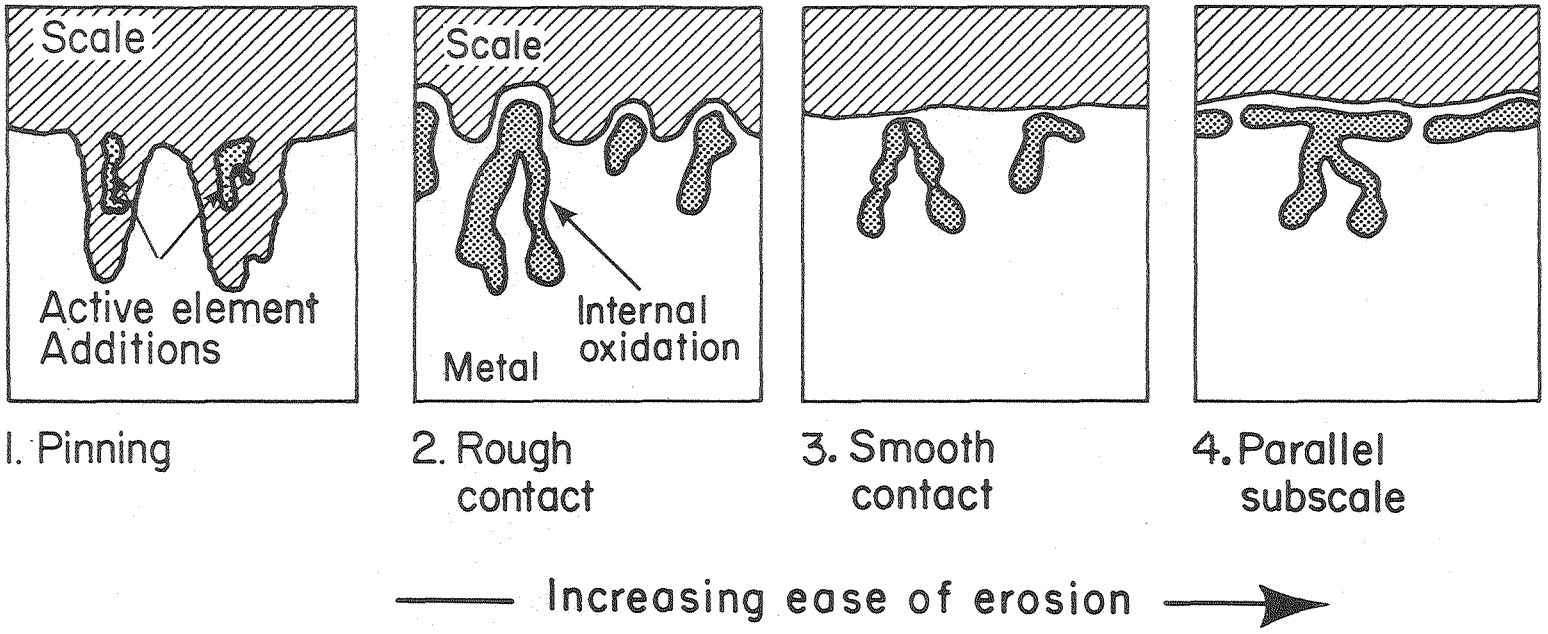

Fig. 12

XBL 7912-13356A

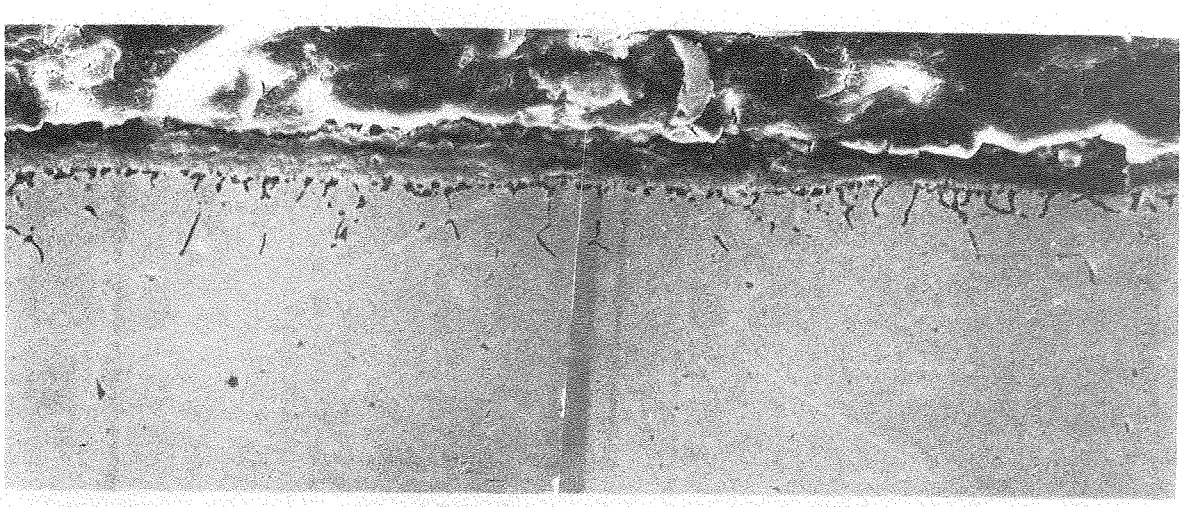

Type 310 S.S.

Oxidized - Sulfidized: Log P_{O_2} = -15, Log P_{S_2} = -6, 1800°F

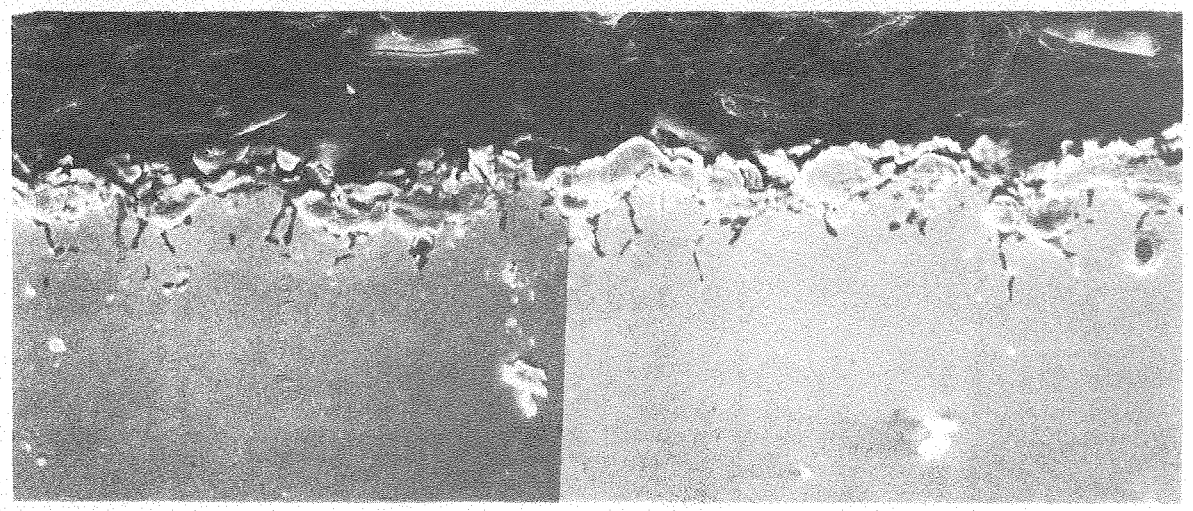

XBB 797-8945

Fig. 13

Type 310 S.S. Preoxidized: Log P_{O_2} = -15, 1800°F

Oxidized - Sulfidized: Log P_{O_2} = -15, Log P_{S_2} = -6, 1800°F

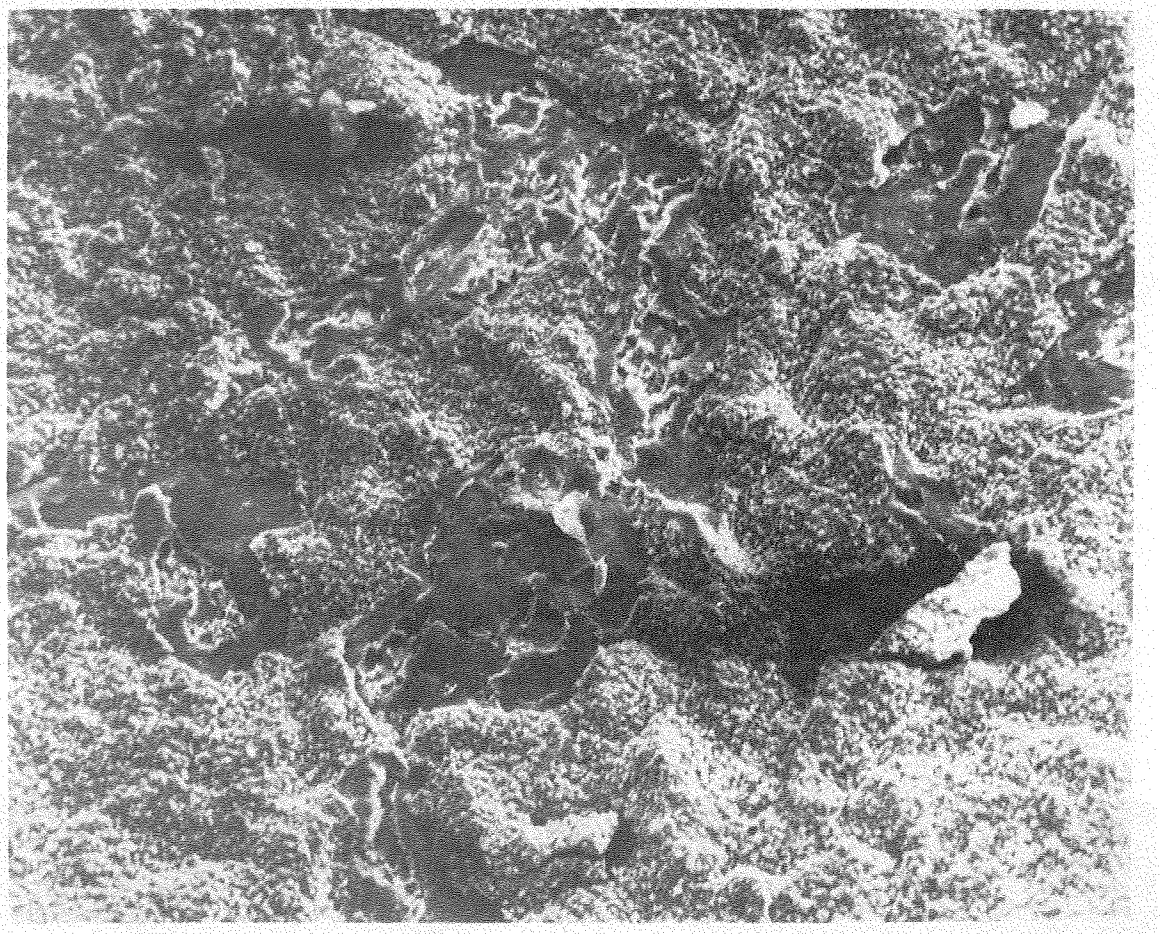

Fig. 14

XBB 808-10079

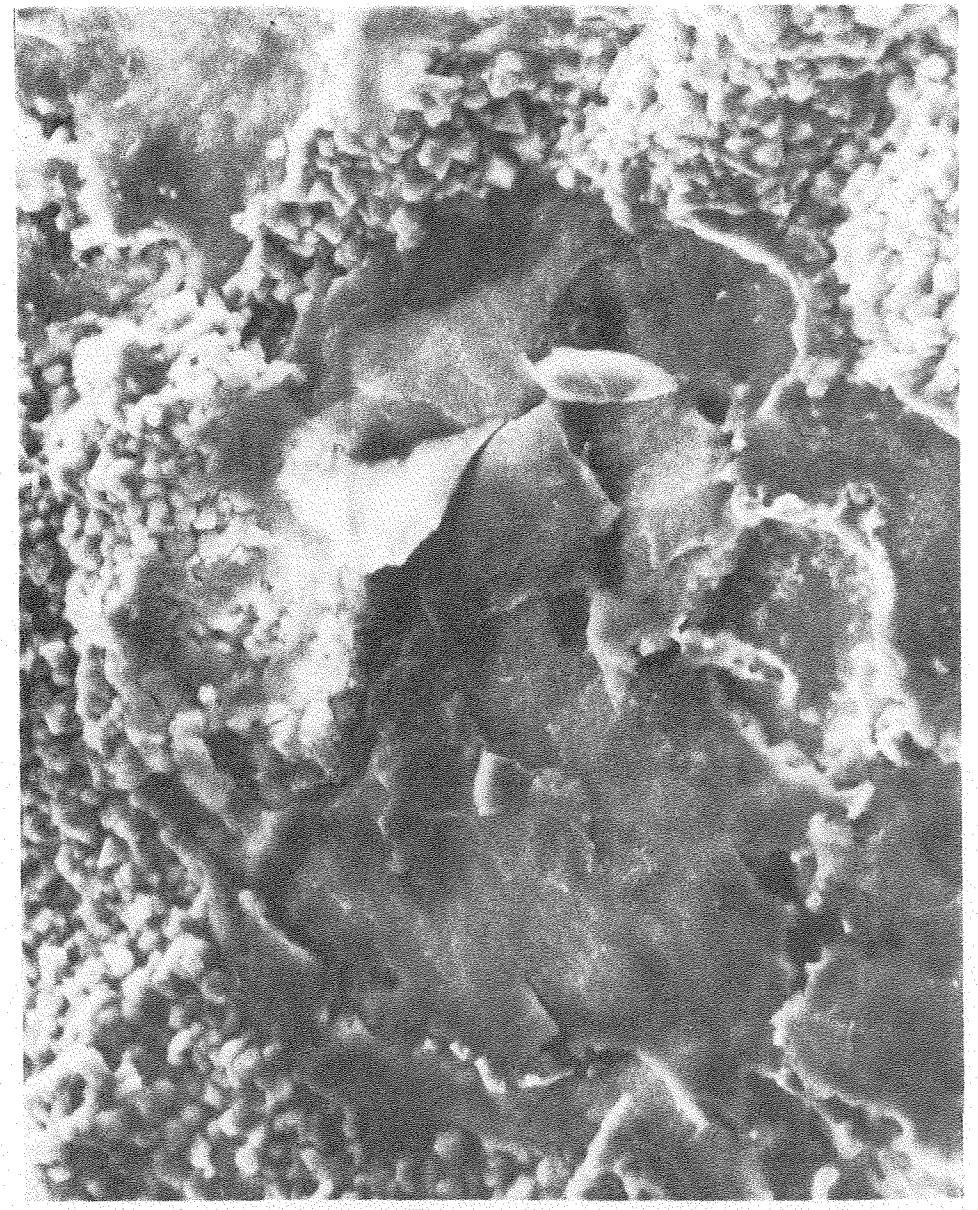

Fig. 15

XBB 808-10078